scientific reports

Check for updates

OPEN

Development of a time-resolved fluorescence-based lateral flow immunoassay for rapid and sensitive diagnosis of Middle East respiratory syndrome

Mi Jeong Kim[1,2,9], Hye-Yeon Kim[3,9], Minhye Kim[1,4], Eun-Young Shin[1], Wooyoung Kim[1,4], Hyunghoon Kim[5], Keun Bon Ku[6], Jong-Hwan Lee[6,7], Seung Il Kim[1,8]✉ & Edmond Changkyun Park[1,4,8]✉

Middle East respiratory syndrome (MERS) is a viral respiratory infection caused by the MERS-coronavirus (MERS-CoV). Due to its high mortality and lack of a vaccine or treatment, MERS has remained on the WHO's priority list of diseases with the highest public health risk since 2012. Although rapid diagnosis is essential for interrupting transmission, initiating timely treatment, and maintaining public health systems, no rapid diagnostic method currently exists for MERS. In this study, a sensitive and specific lateral flow immunoassay (LFIA)-based rapid antigen diagnostic test for MERS was developed using time-resolved fluorescence (TRF) technology. Monoclonal antibodies specific for the MERS-CoV N protein were generated, and optimal pairs were selected through affinity measurement. A TRF-LFIA using Europium nanoparticles was then constructed based on these pairs. The TRF-LFIA showed a detection limit of 0.1 ng/ml MERS-CoV N protein and 5×10^4 copies/ml of MERS-CoV, demonstrating a 25-fold sensitivity increase relative to the cellulose nanobeads (CNB)-LFIA. Furthermore, it displayed high specificity without cross-reactivity to the N proteins of SARS-CoV, SARS-CoV-2, or influenza virus. Consequently, these findings indicate that the TRF-LFIA platform is a promising approach for rapid diagnosis of MERS-CoV infection, with potential for broader application through enhanced sensitivity.

Keywords MERS, Nucleocapsid protein, Rapid diagnostic test, Time-resolved fluorescence, Europium

Middle East respiratory syndrome (MERS), a viral respiratory disease caused by the MERS-coronavirus (MERS-CoV), was first identified in Saudi Arabia in 2012. MERS-CoV (a member of the genus *Betacoronavirus* within the family Coronaviridae) contains a single positive strand RNA genome that encodes four structural proteins: spike, envelope, matrix, and nucleocapsid (N)[1,2]. MERS-CoV is transmitted to humans from infected dromedary camels, and common symptoms of infection include fever, cough, shortness of breath, muscle pain, and sore throat. In severe cases, patients may develop pneumonia, acute respiratory distress syndrome, kidney failure, and even death[3–6]. As of February 2025, there were 2618 laboratory-confirmed MERS cases reported in 27 countries, with 945 deaths (fatality rate, 36%); however, the number of MERS-CoV infections has declined markedly since the onset of the coronavirus disease 2019 (COVID-19) pandemic. This reduction is thought to be associated with

[1]Digital Omics Research Center, Korea Basic Science Institute, Cheongju 28119, Republic of Korea. [2]Immunotherapy Research Center, Korea Research Institute of Bioscience and Biotechnology, Daejeon 34141, Republic of Korea. [3]Biopharmaceutical Research Center, Korea Basic Science Institute, Cheongju 28119, Republic of Korea. [4]Critical Diseases Diagnostics Convergence Research Center, Korea Research Institute of Bioscience and Biotechnology, Daejeon 34141, Republic of Korea. [5]Precision Biosensor, Inc., Daejeon 34036, Republic of Korea. [6]Center for Infectious Disease Vaccine and Diagnosis Innovation, Korea Research Institute of Chemical Technology, Daejeon 34114, Republic of Korea. [7]College of Advanced Technology and Convergence, Major in Bionano Engineering, Hanyang University, Ansan 15588, Republic of Korea. [8]Department of Bio-Analysis Science, University of Science and Technology, Daejeon 34113, Republic of Korea. [9]Mi Jeong Kim and Hye-Yeon Kim contributed equally to this work. ✉email: ksi@kbsi.re.kr; edpark@kbsi.re.kr

nonpharmaceutical interventions implemented to control COVID-19, such as mask-wearing, hand hygiene, and physical distancing, which may have concurrently suppressed MERS-CoV transmission[7]. Despite the decline in the number of MERS cases, the World Health Organization (WHO) expects that additional cases of MERS will be reported in the Middle East, and that the virus will continue to spread internationally[7]. Therefore, early identification of MERS-CoV infection in both community and healthcare settings remains critical for mitigating and controlling potential future outbreaks of MERS.

Although fatal MERS has been prevalent for over a decade, there is still no applicable point-of-care testing (POCT) technology. Currently, real-time quantitative reverse transcription polymerase chain reaction (qRT-PCR) is only commercially available method of detecting MERS-CoV RNA[8]. The high accuracy and low limit of detection (LOD) afforded by nucleic acid amplification tests have established them as the diagnostic gold standard for detecting various pathogens; however, molecular diagnostics require specialized equipment and expensive reagents, with particular reliance on skilled experts for execution and data interpretation. The diagnostic process, from RNA extraction to interpretation of the PCR result, also requires a significant amount of time; therefore, molecular diagnostic technology is not suitable for prompt on-site diagnosis, which enables immediate isolation of patients and limits spread of infection. In contrast, rapid antigen diagnostic tests (RADT), a type of immunological diagnostic technology, are used widely for POCT to diagnose respiratory infectious diseases such as influenza and COVID-19[9]. Despite this, no commercially available RADT exists for MERS. Therefore, the development of a RADT for MERS is essential to ensure preparedness for future outbreaks.

The RADT is based on a typical lateral flow immunoassay (LFIA) platform, which allows visual interpretation through observation of color changes in a strip using the naked eye. Conventional LFIA uses a pair of antibodies to capture an antigenic protein, and gold nanoparticles (AuNP) or colored nanobeads such as cellulose nanobeads (CNB) as a signal detection dye[10,11]. While LFIA delivers diagnostic results within 15 min, the method is not appropriate for early diagnosis during the pre-symptomatic period due to its relatively high LOD. To increase the sensitivity of LFIA, fluorescent dyes such as fluorescein isothiocyanate and quantum dot have been used instead of AuNP[12–15]. However, conventional fluorescent dyes exhibit spectral overlap between the higher wavelength end of the excitation spectrum and the lower wavelength end of the emission spectrum[16,17]. This property generates background signals due to simultaneous excitation and emission, a phenomenon that has a negative impact on assay sensitivity. Additionally, conventional LFIAs typically rely on passive adsorption of antibodies onto nitrocellulose membranes, which often leads to random orientation of the captured antibodies. This non-specific immobilization reduces antigen accessibility and lowers assay reproducibility and sensitivity.

Recent studies revealed that the time-resolved fluorescence (TRF) detection method may have a revolutionarily impact on the sensitivity of LFIA[18–20]. Lanthanide fluorophores, such as Europium, Terbium, and Samarium, emit light with a long decay time. Due to this continuous fluorescence persists for milliseconds, transient fluorescence, which lasts only a few nanoseconds, can be excluded by measuring emission after a certain period of time following excitation by a short pulse of light[21]. This increases the signal-to-noise ratio, thereby enabling more sensitive measurement of the fluorescent signals and, consequently, increasing the overall sensitivity of the assay.

In this study, we developed a TRF-RADT to address the absence of a MERS-specific RADT and the sensitivity limitations of conventional LFIA platforms. To this end, mouse monoclonal antibodies (mAbs) specific for the N protein of MERS-CoV were generated and the most effective sandwich pair was identified for antigen detection. The selected antibody pair was applied to construct a TRF-RADT, in which biotinylated capture antibodies were immobilized via streptavidin to improve binding orientation. The diagnostic performance of the TRF-RADT was then evaluated, as schematically illustrated in Fig. 1. The TRF-RADT demonstrated excellent diagnostic performance and represents a promising tool for the rapid detection of MERS-CoV.

Results and discussion

Antigen preparation and mAb production for MERS-CoV N protein

To develop a RADT for MERS diagnosis, MERS-CoV N protein-specific mouse Abs (mAbs) were initially generated. N protein is known as the second largest structural protein comprising 413 amino acid residues and it binds to the viral RNA genome and induces viral replication and assembly. It is a recognized diagnostic target because its amino acid sequence is highly conserved across coronaviruses[22]. To develop the LFIA-based RADT, two different antibodies are used for the sandwich immunoassay: one for use as a capture antibody and the other for use as a detection antibody. Effective assay performance requires that the two antibodies recognize spatially distinct epitopes. Binding to identical or adjacent epitopes may cause steric hindrance, which reduces the efficiency of antigen–antibody interactions and compromises diagnostic performance.

Therefore, to generate a pair of diagnostic antibodies that recognize spatially distinct epitopes, we divided MERS-CoV N protein antigen into two domains: the NTD (amino acids 1–164, which contain the RNA binding domain) and the CTD (amino acids 168–413, which contain the dimerization domain). Each domain was expressed and purified from *E. coli* (Fig. S1), and the purified recombinant NTD and CTD peptides were used to immunize mice. After isolating B cells from the immunized mice, cell fusion (for hybridoma production) and limiting dilution cloning were performed to select the three most sensitive mAbs for each domain: these were N6E6, N7E9, N8F7 for the NDT, and C4D5, C5G2, C6D2 for the CTD (Fig. 2A).

Subsequently, the specificity of the antibodies against recombinant N proteins of MERS-CoV, SARS-CoV, and SARS-CoV-2 was evaluated using an indirect ELISA. All three mAbs targeting the NTD (N6E6, N7E9 and N8F7) exhibited strong reactivity against the MERS-CoV N protein, with no cross-reactivity to the N protein of SARS-CoV or SARS-CoV-2 (Fig. 2B). Among the mAbs targeting the CTD, only C6D2 interacted specifically with the MERS-CoV N protein. The C4D5 mAb exhibited sensitivity comparable with that of the other mAbs, but it also bound to the SARS-CoV and SARS-CoV-2 N protein. Regarding C5G2, although it exhibited only a weak interaction with the SARS-CoV and SARS-CoV-2 N proteins, it exhibited relatively low sensitivity (Fig. 2B).

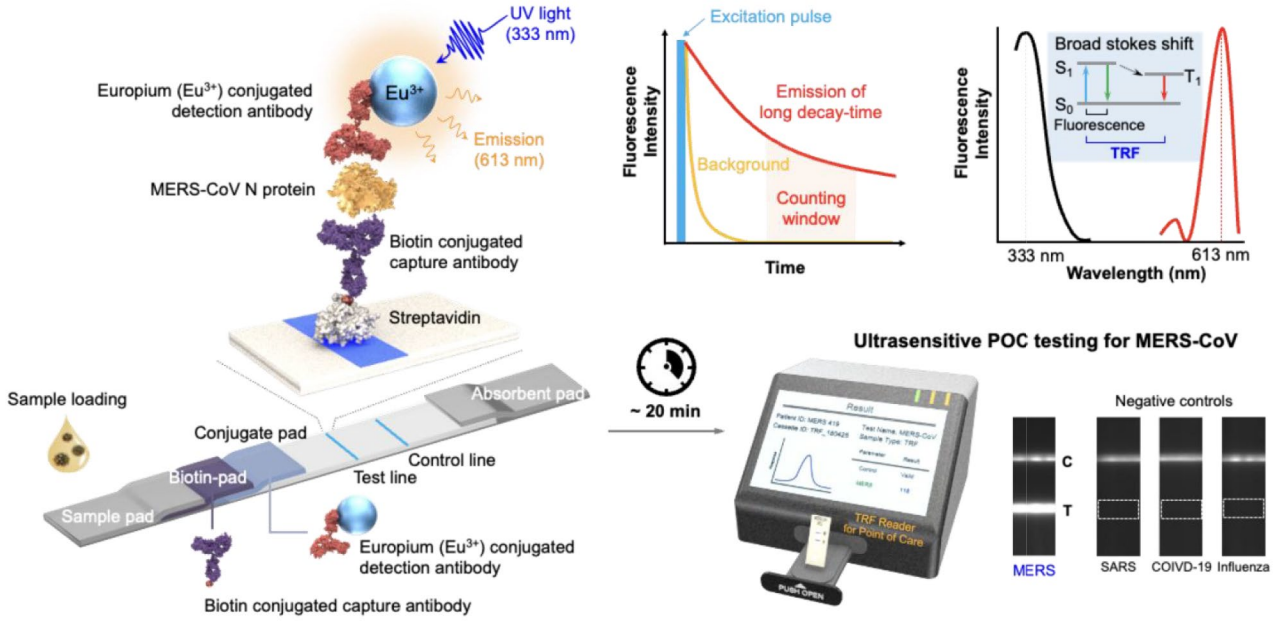

Fig. 1. Schematic overview of the TRF-RADT kit development for rapid and specific MERS-CoV detection. This figure provides a schematic representation of the TRF-RADT kit illustrating its component assembly and diagnostic workflow for the specific detection of MERS-CoV within 20 min without cross-reactivity.

Screening of diagnostic antibody pairs for MERS

To screen the antibody pairs for use in a RADT, all possible combinations of the six mAbs were tested using a direct sandwich ELISA. Capture antibodies were immobilized onto the surface of 96-well plates, and the detection antibodies were directly conjugated to HRP (Fig. 3A). Among the 36 candidate antibody pairs, three combinations (capture-detection: N6E6-C6D2, N7E9-C6D2, and N8F7-C6D2) generated the strongest signals in response to the MERS-CoV N protein (Fig. 3B). No cross-reactivity was observed with N protein from other viruses, including influenza virus (Fig. 3C). Therefore, these three antibody sandwich pairs were selected for specific detection of MERS-CoV. The notable feature of the three selected diagnostic antibody pairs is that one antibody within each pair targets the NTD, while the other targets the CTD, of the MERS-CoV N protein. These results suggest that dividing the antigen into NTD and CTD was an effective strategy for identifying functional antibody pairs.

To evaluate the diagnostic applicability of the selected mAbs, their binding affinities to the MERS-CoV N protein were assessed using a real-time, label-free biolayer interferometry biosensor. As shown in Fig. 3D, the dissociation constants (K_D) of N6E6, N7E9, N8F7, and C6D2 were 0.001, 8.496, 1.589, and 0.001 nM, respectively. The K_D value of one of the commercially available anti-MERS-CoV N protein antibodies was 4.7 nM (data not shown). This indicates that our mAbs have high affinity for the MERS-CoV N protein, making them suitable for use as an LFIA platform for MERS diagnosis.

Application of the diagnostic antibody pairs to the LFIA platform

To evaluate the suitability of the selected antibody pairs for use in RADT, the three selected pairs were tested on the LFIA platform. The capture antibodies (N6E6, N7E9, and N8F7) were immobilized onto the test line of the NC membrane, and the detection antibody (C6D2) was labeled with CNB prior to addition to the conjugation pad (Fig. 4A). The results showed that all the sandwich antibody pairs detected the MERS-CoV N protein antigen specifically, with no significant cross-reactivity with N proteins from SARS-CoV, SARS-CoV-2, or influenza virus (Fig. 4B). The visual detection limit of each pair was as follows: 2.5 ng/ml for the N6E6-C6D2 pair, 5 ng/ml for the N7E9-C6D2 pair, and 10 ng/ml for the N8F7-C6D2 pair (Fig. 4B). To obtain a more objective measurement, the band intensity was analyzed using an LFIA reader. The respective detection limits were 2.5 ng/ml for the N6E6-C6D2 pair, 2.5 ng/ml for the N7E9-C6D2 pair, and 5 ng/ml for the N8F7-C6D2 pair (Fig. 4C). These data confirm that the three selected antibody pairs are suitable for rapid antigen detection on the LFIA platform.

Development of a TRF-LFIA for MERS-CoV

To increase the sensitivity of the CNB-based LFIAs, we substituted the conventional CNBs with Europium chelate nanoparticles as detection probes and employed a biotin-streptavidin system for oriented capture antibody immobilization, thereby enabling the development of a novel TRF-LFIA for MERS-CoV. The LFIA strip comprised a sample pad, a biotin pad containing a capture antibody conjugated to biotin, a conjugation pad containing a detection antibody and chicken IgY conjugated to Europium, an NC membrane containing streptavidin on the test line and anti-chicken IgY antibody on the control line, and an absorbent pad (Fig. 5A).

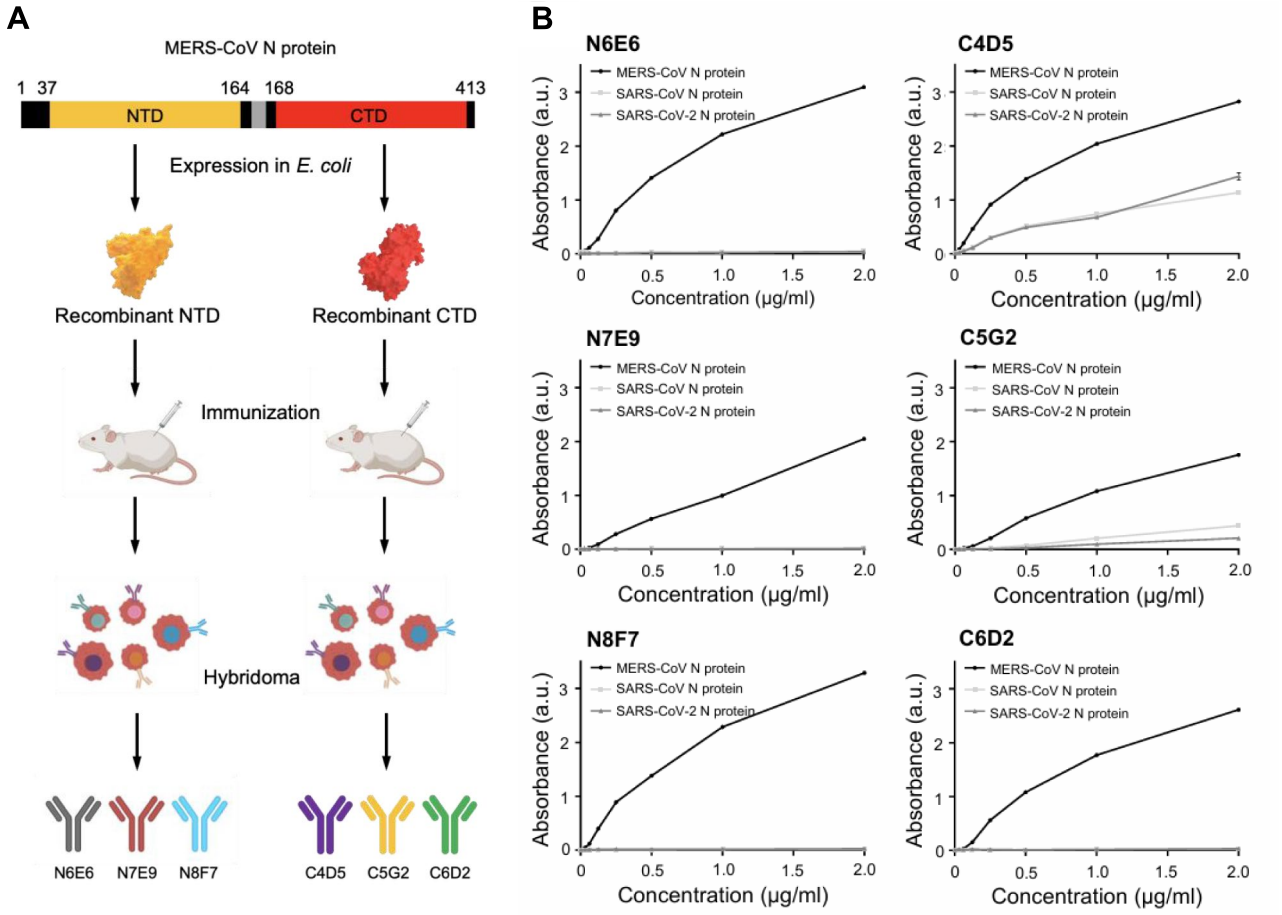

Fig. 2. Production of specific antibodies for MERS-CoV N protein. (**A**) Schematic diagram of procedures for developing mouse mAbs for MERS-CoV N protein. Recombinant NTD and CTD of MERS-CoV N protein were used for mouse immunization and the three most sensitive mAbs for each domain were selected. (**B**) Indirect ELISA results for measuring the sensitivity and specificity of the MERS-CoV N protein mAbs.

When the samples were dropped onto the sample pad, the MERS-CoV N protein in the sample is bound by the biotin-labeled capture antibody, followed by binding to the detection antibody labeled with Europium. This forms an antibody sandwich on the conjugation pad. The resulting analyte is captured by streptavidin on the test line, and the chicken IgY antibodies are captured by the anti-chicken IgY antibody on the control line (Fig. 5A). After 20 min, the fluorescence intensity of the test and control lines can be measured in a portable TRF-LFIA reader.

The detection limits of the TRF-LFIAs using the three antibody pairs were 0.1 ng/ml for N6E6-C6D2 and 1 ng/ml for both N7E9-C6D2 and N8F7-C6D2 (Fig. 5B,C and S2). Thus, the TRF-LFIA based on the N6E6-C6D2 pair was 25-fold more sensitive than the CNB-LFIA. However, the TRF-LFIAs based on the N7E9-C6D2 and N8F7-C6D2 pairs exhibited relatively lower sensitivity, only 2.5-fold and fivefold higher, respectively, than the CNB-LFIA. In terms of selectivity, and similar to the CNB-LFIA, none of the TRF-LFIAs cross-reacted with the N protein from other viruses (Fig. 5B,C and S2). Taken together, these data show that the selected antibody pairs are suitable for use in a TRF-LFIA and demonstrate superior performance compared to the CNB-LFIA. Moreover, the application of TRF technology to the LFIA platform, coupled with the biotin-streptavidin-mediated enhancement of antibody immobilization and assay sensitivity, led to a significant improvement in overall performance.

Detection of MERS virus using the TRF-LFIA

Finally, to confirm the diagnostic performance of the TRF-LFIA, we measured the LOD for cultured virus. The results showed that TRF-LFIA based on the N6E6-C6D2 antibody pair had a LOD of 5×10^4 copies/ml for cultured MERS-CoV (Fig. 6A,C and S3). In fact, the N6E6-C6D2 antibody pair exhibited the highest detection sensitivity for the N protein among the three selected antibody pairs in both the CNB-LFIA and TRF-LFIA formats (Figs. 4C and 5C). In contrast, the TRF-LFIA based on the N7E9-C6D2 and N8F7-C6D2 pairs exhibited higher LOD, at 1×10^7 copies/ml and 1×10^6 copies/ml, respectively (Fig. 6A,C and S3). Additionally, we assessed the LOD of the most effective TRF-LFIA using MERS-CoV-spiked nasal fluid, which served as a surrogate for clinical samples. The assay demonstrated an LOD of 5×10^5 copies/ml (Fig. 6B,D), even without optimization.

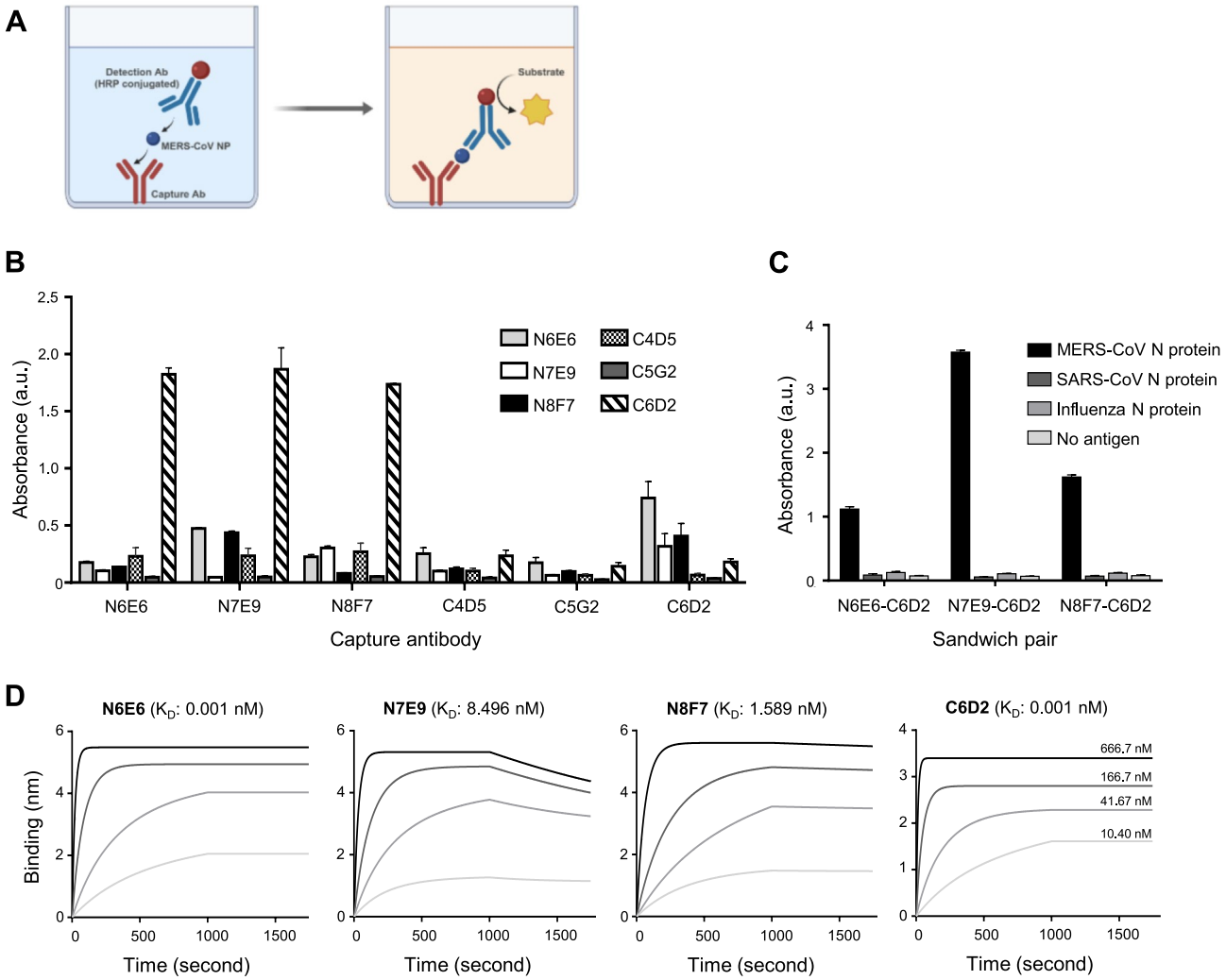

Fig. 3. Identification of diagnostic antibody sandwich pairs for detecting MERS-CoV N protein. (**A**) Schematic diagram of direct sandwich ELISA. (**B**) Direct sandwich ELISA results for screening antibody pairs for detecting MERS-CoV N protein. (**C**) Direct sandwich ELISA results for measuring specificity of the selected antibody pairs. (**D**) The biolayer interferometry results of the selected mAbs against the MERS-CoV N protein. K_D: equilibrium dissociation constant.

The TRF-LFIA platform, as currently configured, demonstrates analytically meaningful sensitivity in both cultured viral samples and surrogate clinical matrices. For its effective translation into diagnostic practice, refinement of key assay parameters such as antibody-antigen binding affinity, bioconjugation strategies, and signal amplification methods may further reduce the detection limit and improve analytical precision. Stability assessments under diverse storage and environmental conditions could provide essential evidence of assay robustness and support real-world deployment. Furthermore, validation using a wide spectrum of patient-derived specimens is also critical to establish diagnostic reliability across biologically diverse backgrounds. Consequently, these refinements are expected to facilitate the advancement of the TRF-LFIA platform into a reliable, scalable, and clinically applicable diagnostic solution.

Conclusion

Rapid diagnosis of MERS is essential for effective disease surveillance, a timely outbreak response, clinical management, and public health preparedness, ultimately contributing to global health security. In this study, a RADT for MERS diagnosis was developed by generating novel MERS-CoV N protein-specific mouse mAbs and identifying optimal diagnostic antibody pairs for use in RADTs. The CNB-based colorimetric LFIA employing these diagnostic antibody pairs successfully detected MERS-CoV N proteins without cross-reacting with the N proteins of other coronaviruses. Furthermore, to increase the sensitivity of the CNB-LFIA, Europium chelate nanoparticles were substituted for CNB as the detection dye. Using this approach, a TRF-LFIA was constructed in which biotinylated capture antibodies were immobilized via streptavidin to improve antibody orientation and binding efficiency. The Europium-based TRF-LFIA exhibited high sensitivity (LOD, 0.1 ng/ml) for the MERS-CoV N protein, and was able to detect 5×10^4 copies/ml of MERS-CoV. Given its high sensitivity in detecting

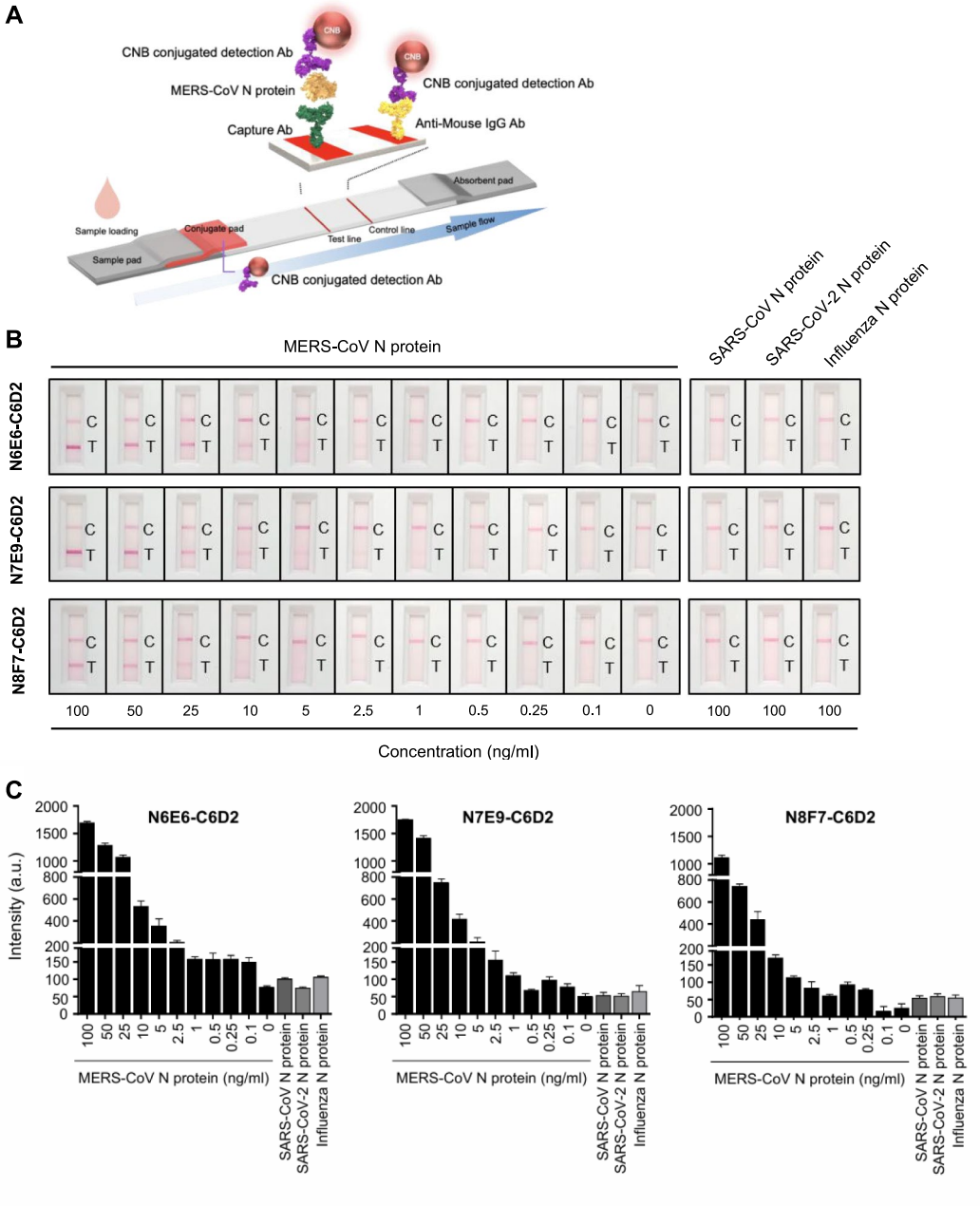

Fig. 4. The detection performance of colorimetric LFIA for the MERS-CoV N protein. (**A**) Schematic diagram of the colorimetric LFIA configuration. (**B**) Representative images of the colorimetric LIFA results with the selected antibody pairs. C: control line, T: test line. (**C**) The bar graph showing intensities of the test line of the colorimetric LIFA. The color intensity was measure by a LIFA reader. The data are average ± standard deviation of three individual experiments.

MERS-CoV-spiked nasal fluid, the TRF-LFIA platform represents a promising approach for MERS diagnosis, with potential applications in epidemiological surveillance and outbreak management.

Materials and methods

Production of N protein antigen

The full-length N gene of MERS-CoV was synthesized and cloned into the pET28a vector harboring an N-terminal 6×His tag. Then, the N-terminal domain (NTD, 1-492 nucleotide) and C-terminal domain (CTD, 502–1239 nucleotide) of the MERS-CoV N gene were subcloned into the pET28a vector, again with an N-terminal 6×His tag. The plasmids were then transformed into *E. coli* BL21(DE3) and expression of the recombinant N proteins was induced by addition of 0.5 mM isopropyl β-D-1-thiogalactopyronoside to the bacterial culture. Bacterial cells were lysed by sonication, and soluble recombinant N proteins were purified by affinity chromatography using a HisTrap™ Fast Flow column (GE HealthCare Technologies, Inc., Chicago, IL, USA). Finally, proteins were

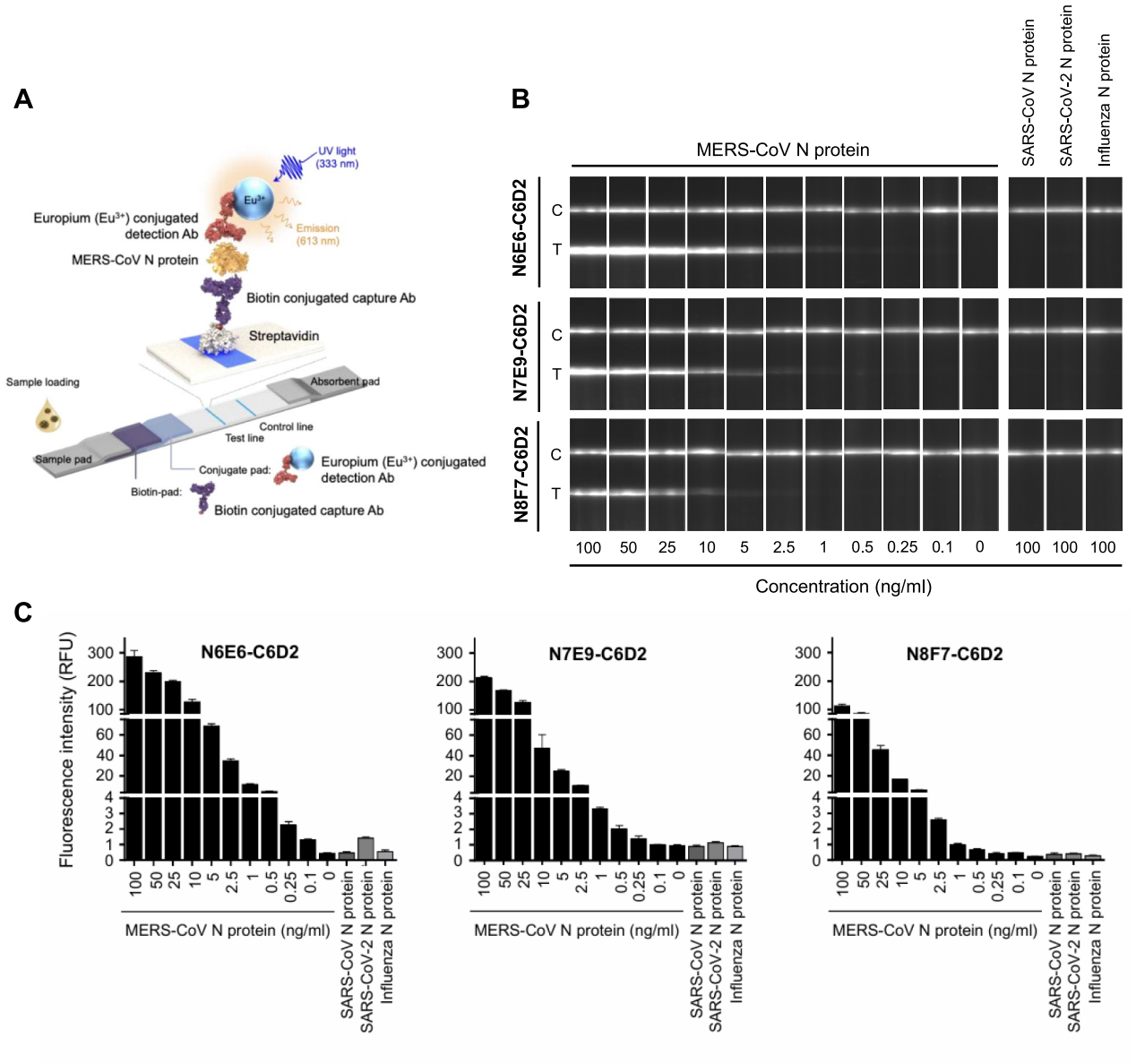

Fig. 5. The detection performance of TRF-LFIA for the MERS-CoV N protein. (**A**) Schematic diagram of the TRF-LFIA configuration. (**B**) Representative images of the TRF-LIFA results with the selected antibody pairs. C: control line, T: test line. The images were taken by a TRF-LFIA reader. (**C**) The bar graph showing fluorescence intensities of the test line of the TRF-LIFA. The fluorescence intensity was measure by the TRF-LFIA reader. The data are average ± standard deviation of three individual experiments.

concentrated to 2 mg/ml in phosphate-buffered saline (PBS). The entire study was reviewed and approved by the Institutional Biosafety Committee (IBC) of the Korea Research Institute of Chemical Technology (KRICT-IBC-2019-004, approved on December 20, 2019).

Production of mouse mAbs

The animal study protocol was approved by the Institutional Animal Care and Use Committee (IACUC) of the Korea Basic Science Institute (Approval number: KBSI-20-18). All animal experiments were conducted in accordance with relevant guidelines and regulations, including those of the IACUC and the ARRIVE guidelines (https://arriveguidelines.org).

The mouse mAbs were produced according to a previous report[23]. In brief, the recombinant proteins were mixed with Freund's adjuvant (Sigma-Aldrich, St. Louis, MO, USA) and injected into BALB/c mice (Orient Bio Inc., Seongnam, Republic of Korea). After immunization, the mouse spleen was harvested and lymphocytes isolated. The lymphocytes were then fused with the Sp2/0-Ag14 myeloma cell line (Catalog No. CRL-1581, ATCC) at a 5:1 ratio using polyethylene glycol (PEG)-1500 (Roche, Basel, Switzerland). The fused cells (hybridomas) were cultured in hypoxanthine, aminopterin, and thymidine (HAT) selection medium (RPMI1640 with HAT

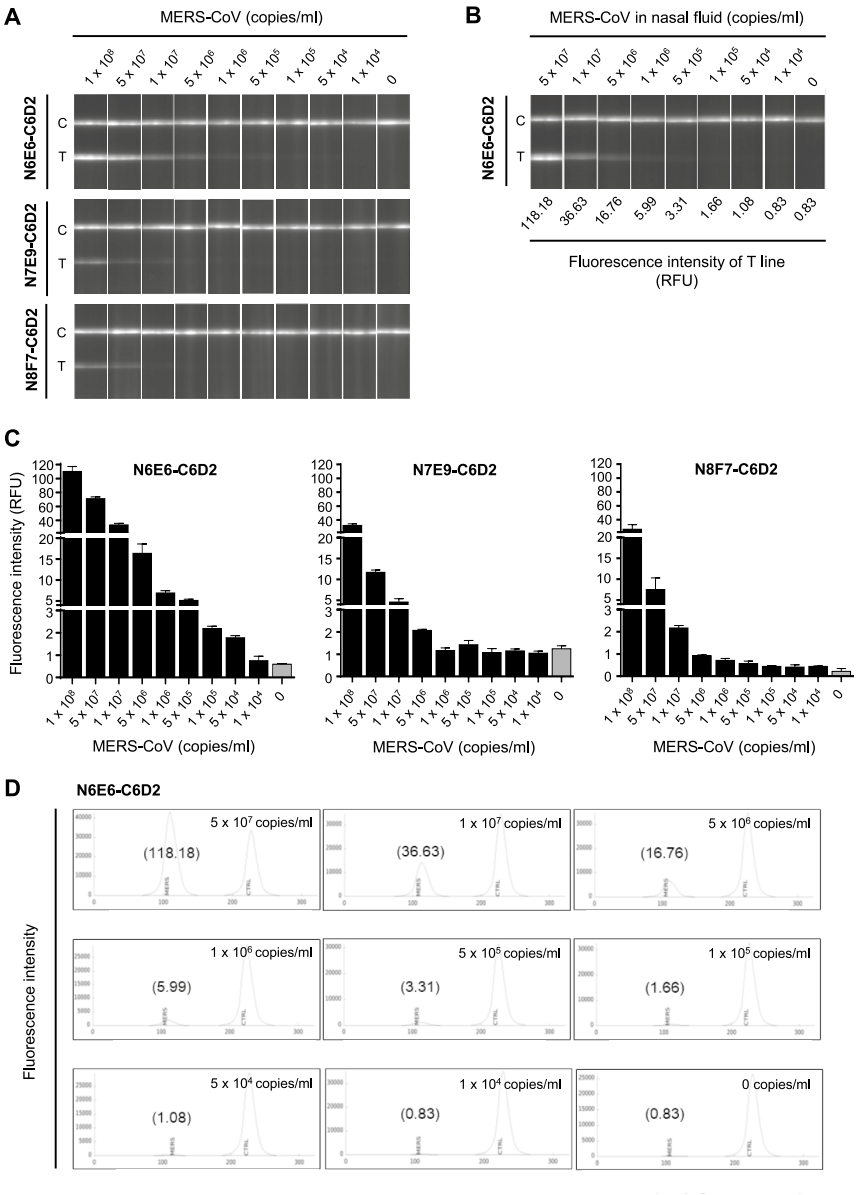

Fig. 6. The detection performance of TRF-LFIA for the MERS-CoV. (**A**) Representative images of the TRF-LIFA results of detecting cultured MERS-CoV. C: control line, T: test line. (**B**) The images of the TRF-LIFA results of detecting cultured MERS-CoV in nasal fluid. (**C**) The bar graph showing fluorescence intensities of the test line of the TRF-LIFA. The fluorescence intensity was measure by the TRF-LFIA reader. The data are average ± standard deviation of three individual experiments. (**D**) The histogram results of Fig. 6B. The fluorescence signal intensity of test line and control line of TRF-LIFA was measured by a TRF strip reader. The number in parentheses represents the intensity value of the test line.

supplement, Catalog No. H0262, Sigma-Aldrich), and single-cell clones of hybridomas were sorted and selected using the limiting dilution method. Subsequently, the hybridoma cells were screened in an indirect enzyme-linked immunosorbent assay (ELISA) to confirm production of antibodies that bind to the specific antigens. Three hybridoma clones specific for each antigen protein were selected. These hybridoma clones were cultured in RPMI 1640 medium, and the antibodies were purified using Protein A Sepharose and SP Sepharose columns.

ELISA

For the indirect ELISA, the N proteins of MERS-CoV, SARS-CoV (Catalog No. 40143-V08B, Sino Biological, Inc., Beijing, China), and SRAS-CoV-2 (Catalog No. 40588-V08B, Sino Biological, Inc.) were immobilized in the wells of 96-well plates for 1 h at room temperature. The plate was then washed three times with Tris-buffered saline containing 0.1% Tween-20 (TBST), and blocked with 5% bovine serum albumin (BSA) in TBST for 1 h at room temperature. The hybridoma culture supernatant or purified mAbs were added to the blocked well for 1 h at room temperature to allow the antibodies to bind to the coated antigens. The plates were then washed

three times with TBST, followed by addition of a horseradish peroxidase (HRP)-conjugated anti-mouse IgG antibody (Catalog No. 7076S, Cell Signaling Technology, Danvers, MA, USA) for 1 h at room temperature. After extensive washing with TBST, a tetramethylbenzidine (TMB) substrate (Thermo Fisher Scientific, Waltham, MA, USA) was added to develop the color signal. The reaction was stopped by addition 1 M sulfuric acid (Samchun Chemicals, Seoul, Republic of Korea), followed by measurement of the signal in a microplate reader (SpectraMax M4, Molecular Devices, San Jose, CA, USA).

For the direct sandwich ELISA, the capture antibodies were immobilized in the wells of a 96-well plate for 1 h at room temperature. The plate was then washed three times with TBST and blocked with 5% BSA in TBST for 1 h at room temperature. The N proteins were added to the well for 1 h at room temperature to allow antigens to bind to the coated capture antibodies. The plates were then washed three times with TBST, followed by addition of an HRP-conjugated detection antibody for 1 h at room temperature. The purified detection mAb was labeled with HRP using the EZ-Link™ Activated Peroxidase Antibody Labeling Kit (Catalog No. 31497, Thermo Fisher Scientific). The plate was then washed and TMB added to develop the color signals, which was then measured in a microplate reader.

Measurement of antigen–antibody binding affinity

The affinity of anti-MERS-CoV N protein mAbs for the MERS-CoV N protein was evaluated using biolayer interferometry (BLI) on a BLItz instrument (ForteBio, Fremont, CA, USA) equipped with nickel-coated NTA biosensors (ForteBio, Part No. 18-5102). All BLI procedures were conducted using ForteBio Kinetic Buffer (PBS containing 10 mM phosphate, 150 mM NaCl, 0.1% BSA, and 0.02% Tween-20, pH 7.4), as the assay buffer.

Prior to use, NTA biosensor tips were hydrated in kinetic buffer for 10 min. Kinetic measurements consisted of five sequential steps: (1) baseline acquisition in assay buffer for 30 s; (2) antigen immobilization onto the biosensor surface for 600 s; (3) baseline re-establishment in assay buffer for 120 s; (4) association with anti-MERS-CoV N protein mAbs at serially diluted concentrations for 600 s; and (5) dissociation in assay buffer for 300 s. The MERS-CoV N protein was immobilized at a concentration of 0.1 mg/ml during the loading step, and monoclonal antibodies were tested at various concentrations (10.4, 41.67, 166.7, and 666.7 nM).

BLI data were analyzed using BLItz Pro software (v1.3.0.5, ForteBio). Kinetic parameters, including the equilibrium dissociation constant (K_D), association rate constant (K_{on}), dissociation rate constant (K_{off}), and coefficient of determination (R^2), were determined using global fitting to a 1:1 binding model. Interaction curves were exported from BLItz Pro.

Preparation of a colorimetric LFIA

The LFIA strip comprises a sample pad, a conjugate pad, a nitrocellulose (NC) membrane, and an absorbent pad. To prepare the conjugation pad, the detection antibody was conjugated to colored cellulose nanobeads (CNB, NanoAct™, Asahi Kasei, Japan). The conjugate pad was then soaked in 0.1% Triton X-100 and dried for 1 h at 37 °C. Next, the CNB-conjugated detection antibody was sprayed on the conjugate pad and allowed to dry for 1 h at 37 °C in a vacuum drying oven. The capture antibody (1 mg/ml) and anti-mouse IgG antibody (0.5 mg/ml; Catalog No. ab97261, Abcam, Cambridge, UK) were dispended onto the test and control lines of the NC membrane, which was attached to a backing card, using a line dispenser (ZX1010™, BioDot, Inc., Irvine, CA USA) at a speed of 50 mm/s and a rate of 0.5 µl/cm. After dispensing the antibodies, the NC membrane was dried for 1 h at 37 °C and then blocked with PBS containing 1% BSA for 1 h at 37 °C in a vacuum drying oven. The LFIA was then assembled and the LFIA sheet was cut to a width of 38 mm. Finally, the LFIA strip was housed in a plastic cassette. For the test, 100 µl of sample was applied to the sample pad and the intensity of the test line was measured in an LFIA reader (Wells Bio, Seoul, Republic of Korea).

Preparation of the TRF-LFIA

The TRF-LFIA strip comprises a sample pad, a biotin pad, a conjugate pad, an NC membrane, and an absorbent pad. To prepare the biotin pad, 1 ml of capture antibody solution (4 mg/ml in 50 mM of sodium phosphate buffer (SPB), pH7.5) was mixed with 66 µl of EZ-Link™ Sulfo-NHS-Biotin solution (10 mM in DMSO, Thermo Fisher Scientific) and allowed to react for 1 h at room temperature. The resulting solution was then dialyzed overnight against 100 mM SPB using SnakeSkin™ dialysis tubing (Thermo Fisher Scientific). The biotinylated antibody (0.5% in a printing buffer comprising 1.0% casein, 40 mM EDTA, 0.3% glucose, 1.0% trehalose, and 20 mM SPB, pH 7.5) was sprayed onto a glass fiber strip measuring 1 cm × 30 cm (i.e., the biotin pad) using a spray machine (MDI010, Zeta, Gunpo, Republic of Korea). Finally, the strip was freeze-dried for 4 h.

To prepare the conjugate pad, the detection antibody was conjugated with Europium chelate particles (FluoroMax™ Fluorescent Carboxylate-Modified Particles, 0.2 µm; Thermo Fisher Scientific) using EDC (1-ethyl-3-(3-dimethylaminopropyl) carbodiimide hydrochloride)/Sulfo-NHS (N-hydroxy succinimide esters) coupling chemistry. Briefly, 0.5 ml of Europium particles was washed twice with 50 mM MES (2-(N-Morpholino) ethanesulfonic acid hydrate) buffer (pH 6.1) and collected by centrifugation (12,000 rpm, 30 min). They were then activated by adding 70 µl of EDC solution (10 mg/ml in 50 mM MES) and 140 µl of Sulfo-NHS solution (50 mg/ml in 50 mM MES). This mixture was incubated for 10 min at room temperature with mild agitation on rotary shaker, followed by removal of excess reagents by centrifugation. The pellet comprising activated Europium particles was resuspended in 1 ml of MES buffer. For conjugation to the detection antibody, 1 ml of Europium particle solution was mixed with 0.4 mg of detection antibody solution and incubated for 60 min at room temperature with mild agitation. After removing excess reagents by centrifugation, the particle solution was incubated with 1% BSA (100 mM SPB, pH 7.5) to block unreacted active groups on the Europium particles. After centrifugation, the final collected pellet was dispersed in 5 ml of storage buffer (0.5% BSA, 5% glycerol, 0.025% sodium azide in 10 mM phosphate buffer), which was then added into printing buffer to yield a concentration of 5% (v/v). This was then sprayed onto the 1 cm × 30 cm glass fiber strip (Catalog No. 9254,

Lydall, Inc., Manchester, CT, USA) using a spray machine (DMI010, Zeta, Korea), followed by freeze-drying for 4 h. The same conjugation procedure was performed using a chicken IgY antibody (Catalog No. ABGAC-0500, Arista Biological, Allentown, PA, USA) for use as the control line.

The NC membrane (UniSart® CN140 backed, Sartorius, Göttingen, Germany) has one test line and one control line on which the streptavidin (SA10, Agilent, Santa Clara, CA, USA) and control antibody (anti-chicken IgY, Catalog No. AGCIC-0100, Arista Biological), respectively, are immobilized. Briefly, 500 µl of 1% glutaraldehyde (100 mM SPB, pH 6.8) was mixed with 10 ml of 0.01% streptavidin solution (100 mM SPB, pH 6.8) and allowed to react for 20 min at room temperature. The resulting solution was dialyzed overnight at 4℃ against 10 mM SPB to remove any unreacted reagents. The streptavidin solution was then printed onto the membrane using the dispensing machine (LDAI-601, ZETA). In addition, 0.7 mg/ml of control anti-chicken IgY was dispensed simultaneously onto the membrane at a distance of 4 mm from the test line.

The TRF-LFIA strip was designed to include an additional 1.3 cm × 30 cm glass fiber pad, the function of which is to absorb the specimen (i.e., the sample pad), and a 1.3 cm × 30 cm adsorbent pad (cotton lint fiber, Catalog No. 222, BoreDa Biotech, Seongnam, Republic of Korea). The prepared sample pad, biotin pad, conjugate pad, and adsorbent pad were then laminated onto the NC membrane along with a plastic backing card, and the assembled sheet was cut into a single strip measuring 4.5 mm × 60 mm (width × length) using a guillotine cutting machine (AR-350CG, Artrobo, Namyangju, Republic of Korea). Finally, the strip was placed into a plastic cassette.

For the test, 100 µl of sample was applied to the sample pad and the fluorescence intensity of the test and control lines was measured in a Exdia TRF Plus fluorescence immunoassay analyzer (Precision Biosensor, Inc., Daejeon, Republic of Korea), which utilizes the large Stokes' shift and long decay time of the Europium chelate as an optical probe. The apparatus controls the time-gated acquisition of the Europium fluorescence signal using an ultraviolet LED light source and a CCD camera.

Preparation of inactivated virus samples for diagnostic testing

Virus infection experiments were performed in a biosafety level 3 laboratory. Huh-7 cells were infected with a MERS-CoV (MERS-CoV/KOR/KNIH/002_05_2015, GenBank accession No. KT029139, provided by Korea Disease Control and Prevention Agency) for 48 h, after which the medium containing mature infectious virions was collected. The viral titer was measured in a plaque assay. The harvested virus was inactivated by heating at 100 °C for 15 min. This thermal treatment completely disrupts the viral structure, thereby exposing the nucleocapsid (N) protein for downstream detection. For assay development and performance validation, the inactivated viral lysate was diluted using a lysis buffer (1 × PBS, 1% BSA, 0.6% Tween-20, pH 7.4,). Additionally, to mimic clinically relevant sample conditions, the inactivated virus was spiked into commercially available pooled human nasal fluid, followed by dilution with the same lysis buffer. All prepared samples were stored at − 80 °C until further use.

Data availability

The data used in this study will be made available upon request by the corresponding author.

Received: 29 April 2025; Accepted: 30 June 2025
Published online: 25 July 2025

References

1. Groot, R. J. D. et al. Commentary: Middle East respiratory syndrome coronavirus (MERS-CoV): Announcement of the coronavirus study group. *J. Virol.* **87**, 7790–7792. https://doi.org/10.1128/jvi.01244-13 (2013).
2. Durai, P., Batool, M., Shah, M. & Choi, S. Middle East respiratory syndrome coronavirus: Transmission, virology and therapeutic targeting to aid in outbreak control. *Exp. Mol. Med.* **47**, e181–e181. https://doi.org/10.1038/emm.2015.76 (2015).
3. Assiri, A. et al. Epidemiological, demographic, and clinical characteristics of 47 cases of Middle East respiratory syndrome coronavirus disease from Saudi Arabia: A descriptive study. *Lancet. Infect. Dis.* **13**, 752–761. https://doi.org/10.1016/S1473-3099(13)70204-4 (2013).
4. Yeung, M.-L. et al. MERS coronavirus induces apoptosis in kidney and lung by upregulating Smad7 and FGF2. *Nat. Microbiol.* **1**, 16004. https://doi.org/10.1038/nmicrobiol.2016.4 (2016).
5. Alsaad, K. O. et al. Histopathology of Middle East respiratory syndrome coronovirus (MERS-CoV) infection: Clinicopathological and ultrastructural study. *Histopathology* **72**, 516–524. https://doi.org/10.1111/his.13379 (2018).
6. WHO. *Middle East respiratory syndrome coronavirus (MERS-CoV): Symptoms*, https://www.who.int/health-topics/middle-east-respiratory-syndrome-coronavirus-mers#tab=tab_2 (2024).
7. WHO. *Middle East respiratory syndrome coronavirus - Kingdom of Saudi Arabia*, https://www.who.int/emergencies/disease-outbreak-news/item/2025-DON560 (2025).
8. Kelly-Cirino, C., Mazzola, L. T., Chua, A., Oxenford, C. J. & Kerkhove, M. D. V. An updated roadmap for MERS-CoV research and product development: focus on diagnostics. *BMJ Glob. Health* **4**, e001105. https://doi.org/10.1136/bmjgh-2018-001105 (2019).
9. Fernandes, R. S. et al. Recent advances in point of care testing for COVID-19 detection. *Biomed. Pharmacother.* **153**, 113538. https://doi.org/10.1016/j.biopha.2022.113538 (2022).
10. Budd, J. et al. Lateral flow test engineering and lessons learned from COVID-19. *Nat. Rev. Bioeng.* **1**, 13–31. https://doi.org/10.1038/s44222-022-00007-3 (2023).
11. Kim, J. et al. A two-colour multiplexed lateral flow immunoassay system to differentially detect human malaria species on a single test line. *Malar. J.* **18**, 313. https://doi.org/10.1186/s12936-019-2957-x (2019).
12. Agarwal, S. et al. Lateral flow–based nucleic acid detection of SARS-CoV-2 using enzymatic incorporation of biotin-labeled dUTP for POCT use. *Anal. Bioanal. Chem.* **414**, 3177–3186. https://doi.org/10.1007/s00216-022-03880-4 (2022).
13. Ma, L. et al. Comparison between gold nanoparticles and FITC as the labelling in lateral flow immunoassays for rapid detection of Ralstonia solanacearum. *Food Hydrocolloids* **29**, 1074–1085. https://doi.org/10.1080/09540105.2018.1510474 (2018).
14. Wang, J. et al. Quantum dot-based lateral flow test strips for highly sensitive detection of the tetanus antibody. *ACS Omega* **4**, 6789–6795. https://doi.org/10.1021/acsomega.9b00657 (2019).

15. Liang, Z.-Y., Deng, Y.-Q. & Tao, Z.-Z. A quantum dot-based lateral flow immunoassay for the rapid, quantitative, and sensitive detection of specific IgE for mite allergens in sera from patients with allergic rhinitis. *Anal. Bioanal. Chem.* **412**, 1785–1794. https://doi.org/10.1007/s00216-020-02422-0 (2020).
16. Yeo, S.-J. et al. Improvement of a rapid diagnostic application of monoclonal antibodies against avian influenza H7 subtype virus using Europium nanoparticles. *Sci. Rep.* **7**, 7933. https://doi.org/10.1038/s41598-017-08328-9 (2017).
17. Ou, X. et al. AIEgens assisted label free DNA supersandwich immunoassay for ultrasensitive α-fetoprotein detection. *Giant* **11**, 100110. https://doi.org/10.1016/j.giant.2022.100110 (2022).
18. Lu, J. et al. A time-resolved fluorescence lateral flow immunoassay for rapid and quantitative serodiagnosis of Brucella infection in humans. *J. Pharm. Biomed. Anal.* **200**, 114071. https://doi.org/10.1016/j.jpba.2021.114071 (2021).
19. Lee, M. et al. A comprehensive Exdia TRF-LFIA for simultaneous quantification of GFAP and NT-proBNP in distinguishing ischemic and hemorrhagic stroke. *Clin. Chim. Acta* **557**, 117872. https://doi.org/10.1016/j.cca.2024.117872 (2024).
20. Jiao, X. et al. Lateral flow immunoassay based on time-resolved fluorescence microspheres for rapid and quantitative screening CA199 in human serum. *Int. J. Mol. Sci.* **23**, 9991. https://doi.org/10.3390/ijms23179991 (2022).
21. Natarajan, S., Saatçi, E. & Joseph, J. Development and evaluation of europium-based quantitative lateral flow immunoassay for the chronic kidney disease marker cystatin-C. *J. Fluoresc.* **32**, 419–426. https://doi.org/10.1007/s10895-021-02886-y (2022).
22. Chang, C. K., Hou, M. H., Chang, C. F., Hsiao, C. D. & Huang, T. H. The SARS coronavirus nucleocapsid protein–forms and functions. *Antiviral. Res.* **103**, 39–50. https://doi.org/10.1016/j.antiviral.2013.12.009 (2014).
23. Lee, J. H. et al. Rapid biosensor of SARS-CoV-2 using specific monoclonal antibodies recognizing conserved nucleocapsid protein epitopes. *Viruses* **14**, 255. https://doi.org/10.3390/v14020255 (2022).

Acknowledgements

This work was supported by a grant from National Research Council of Science and Technology, Republic of Korea (Grant Number: CRC22021-100), the Ministry of Health and Welfare, Republic of Korea (Grant Number: HI20C0363), and the Korea Basic Science Institute (Grant Number: C523400).

Author contributions

Mi Jeong Kim: Investigation, Writing—original draft. Hye-Yeon Kim: Conceptualization, Methodology, Investigation. Minhye Kim: Investigation. Eun-Young Shin: Investigation. Wooyoung Kim: Investigation. Hyunghoon Kim: Investigation. Keun Bon Ku: Investigation. Jong-Hwan Lee: Visualization. Seung Il Kim: Funding acquisition, Project administration, Supervision, Writing—review and editing. Edmond Changkyun Park: Conceptualization, Project administration, Supervision, Writing—original draft, review and editing.

Declarations

Competing interests

The authors declare no competing interests.

Additional information

Supplementary Information The online version contains supplementary material available at https://doi.org/10.1038/s41598-025-09832-z.

Correspondence and requests for materials should be addressed to S.I.K. or E.C.P.